

Energy-Tunable Photocatalysis by Hot Carriers Generated by Surface Plasmon Polaritons

Wonmi Ahn,¹ Igor Vurgaftman,² Jeremy J. Pietron,³ Pehr E. Pehrsson,³ and Blake S. Simpkins^{3,}*

¹National Research Council Postdoctoral Associate, U.S. Naval Research Laboratory,
Washington, DC 20375, United States, ²Optical Sciences Division, U.S. Naval Research
Laboratory, Washington, DC 20375, United States, ³Chemistry Division, U.S. Naval Research
Laboratory, Washington, DC 20375, United States

Electronic Supplementary Information

Experimental Photon-to-Carrier Conversion Efficiency in a Ag/TiO₂ Heterofilm.

Calculation of Hole Conversion Efficiency using a Schottky Transport Model.

Supporting Figures

Figure S1. SPP dispersion curve of a bare Au film.

Figure S2. Angle-dependent photocurrents measured in a Ag/TiO₂ heterofilm with varied excitation energies.

Figure S3. Solution pH-dependent photovoltage in a bare Au film.

Figure S4. Cyclic voltammetry curves of a bare Au film.

Figure S5. Dependence of photocurrents on solution pH and electrode potential in a bare Au film.

Experimental Photon-to-Carrier Conversion Efficiency in a Ag/TiO₂ Heterofilm. Photon-to-carrier conversion efficiency (η) was calculated by taking a ratio between the photocurrents measured from a Ag/TiO₂ heterofilm and the illumination intensities of light sources used in each measurement (Eqn. S1). To derive the efficiency in units of electrons per photons, photocurrents were converted to electron fluxes by dividing by the electron charge ($1 e = 1.602 \times 10^{-19} C$). The illumination intensities of LED or laser sources measured using a power meter were converted to photon fluxes by dividing by the photon energy (E , Joules per photon).

$$\eta = \frac{\text{Photocurrent (electrons/sec)}}{\text{Illumination intensity (photons/sec)}} \times 100 \quad (\text{Eqn. S1})$$

Table S1. Photon-to-hot carrier conversion efficiency of a Ag/TiO₂ heterofilm using various light sources (data shown in Figure 2b as solid circles).

Light sources, Energy (eV)		Photocurrent (A)	Illumination intensity (W)	Efficiency (%)
LED	2.4	9.2×10^{-10}	7.9×10^{-6}	2.8×10^{-2}
Laser	2.3	6.2×10^{-10}	1.3×10^{-5}	1.1×10^{-2}
LED	2.1	2.0×10^{-11}	2.5×10^{-6}	1.7×10^{-3}
LED	2.0	6.9×10^{-12}	2.4×10^{-6}	5.7×10^{-4}
LED	1.9	7.4×10^{-12}	9.9×10^{-6}	1.4×10^{-4}
LED	1.7	2.7×10^{-12}	1.1×10^{-5}	4.0×10^{-5}
Laser	1.6	1.4×10^{-11}	3.2×10^{-3}	7.0×10^{-7}

Calculation of Hole Conversion Efficiency using a Schottky Transport Model. The expected efficiency of converting incident photons to carriers in the TiO₂ layer is calculated by integrating the product of the distribution function for the hot-hole generation, the transport efficiency, and the transmission probability at the Ag/TiO₂ interface, assuming momentum conservation parallel to the interface over the hole energies and momentum directions with respect to the interface. The distribution of the generated carriers is assumed to follow the product of the densities of states of the initial and final states:^{1,2}

$$P_g(E) = \frac{g(E)g(E + \hbar\omega)}{\int_{E_F - \hbar\omega}^{E_F} dE' g(E')g(E' + \hbar\omega)} = \frac{\sqrt{E}\sqrt{E + \hbar\omega}}{\int_{E_F - \hbar\omega}^{E_F} dE' \sqrt{E'}\sqrt{E' + \hbar\omega}}$$

where the density of states has the free-particle form $g(E) \propto \sqrt{E}$. The transport efficiency of the hot carriers generated from the decay of SPPs has the following form:³

$$P_T(E) = \frac{1}{L_{SPP}} \int dz e^{-z/L_{SPP}} e^{-z/L_{MFP}(E)} \approx \frac{1}{1 + L_{SPP}/L_{MFP}(E)}$$

where L_{SPP} is the decay length of the SPP mode into the metal, and L_{MFP} is the energy-dependent mean free path of the generated hot holes.⁴

The transmission probability for a hole to be injected over a barrier with height E_B is:⁶

$$T(E, k_y) = \frac{4k_{x,m}k_{x,s}}{(k_{x,m} + k_{x,s})^2}$$

where k_y is the wavevector parallel to the interface (assumed to be the same in the metal and in the TiO₂), $k_{x,m}$ and $k_{x,s}$ are the wavevectors perpendicular to the interface in the metal and in the TiO₂, respectively, that implicitly depend on both E and k_y . The transmission probability becomes low when the effective masses in the metal and the semiconductor are very different, by

analogy with transmission of light at an interface with a refractive index step. The total probability of hole injection is calculated using the expression:

$$P_i(\hbar\omega) = \frac{1}{2} \int_{E_F - \hbar\omega}^{E_B} dE P_g(E) P_T(E) \int \sin \theta(k_y) d\theta(k_y) T(E, k_y)$$

While conservation of k_y can be relaxed to some extent if interface roughness is present (and usually raises the injection efficiency), this effect was not considered in this work.

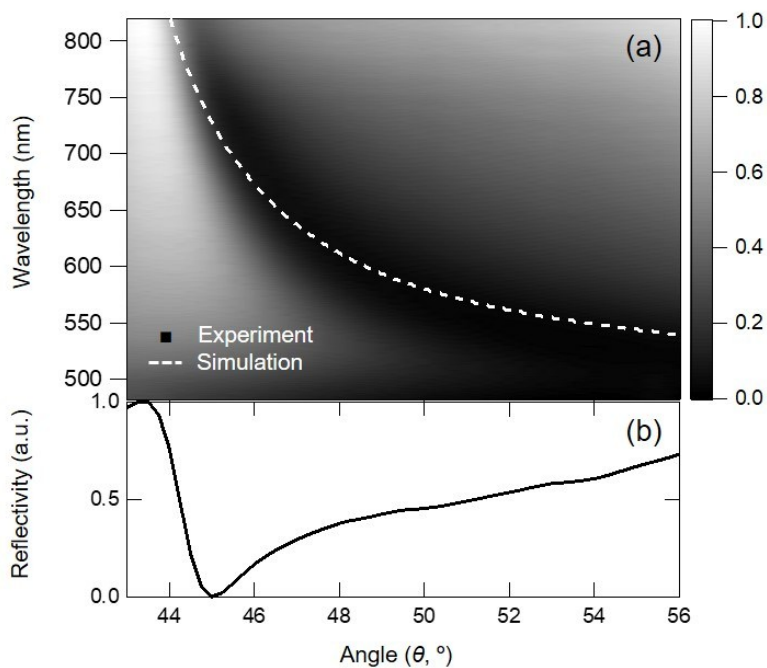


Figure S1. SPP dispersion curve of a bare Au film. (a) SPP dispersion curve measured (black and white contour) and simulated (white dashed line) for a 40 nm-thick Au film (no TiO₂ layer) as a function of an incident angle of light and wavelength. (b) Angle-dependent reflectivity spectrum measured at 785 nm showing an SPP resonant angle at 45°.

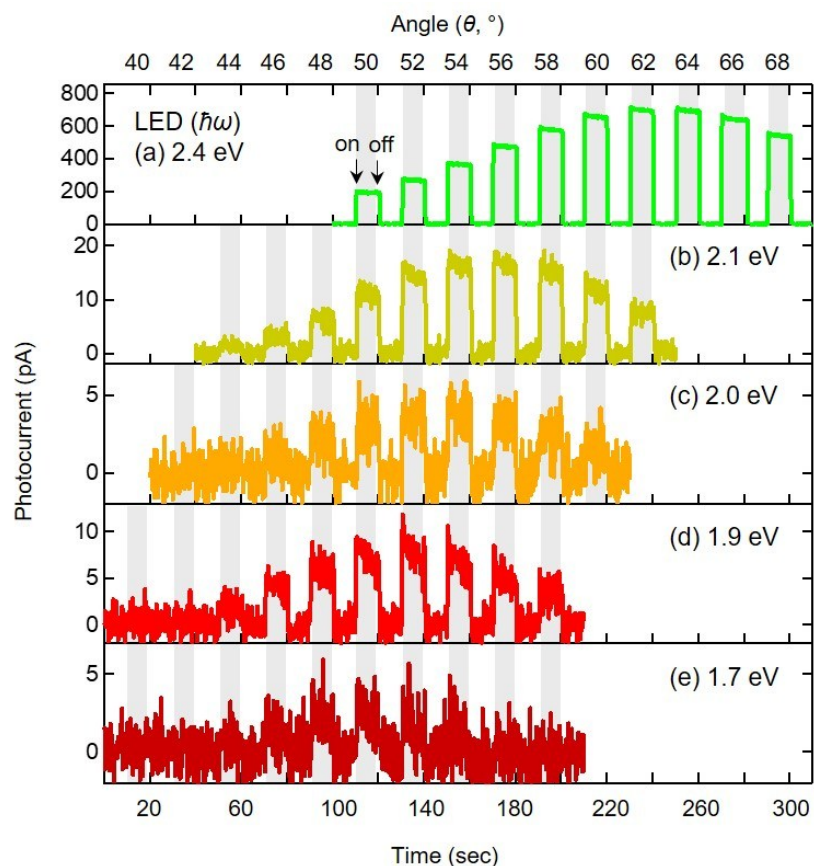


Figure S2. Angle-dependent photocurrents measured in a Ag/TiO₂ heterofilm with varied excitation energies. The Ag/TiO₂ heterofilm was interfaced with a solution of NaOH and CH₃OH. Five different LED sources were used ($\hbar\omega = 2.4$ to 1.7 eV) with an illumination angle of the beam tuned from 40 to 68°. Effective LED powers on the Ag/TiO₂ heterofilm was varied from 2.4 to 11.2 μ W. Gray shaded areas indicate light illumination and white background areas dark conditions (light turned off). A strong angle dependence in photocurrents confirmed SPP-driven hot carrier chemistry. Anodic photocurrents correspond to holes transported from the Ag/TiO₂ working electrode and captured by electron donors in the solution, driving an oxidation reaction.

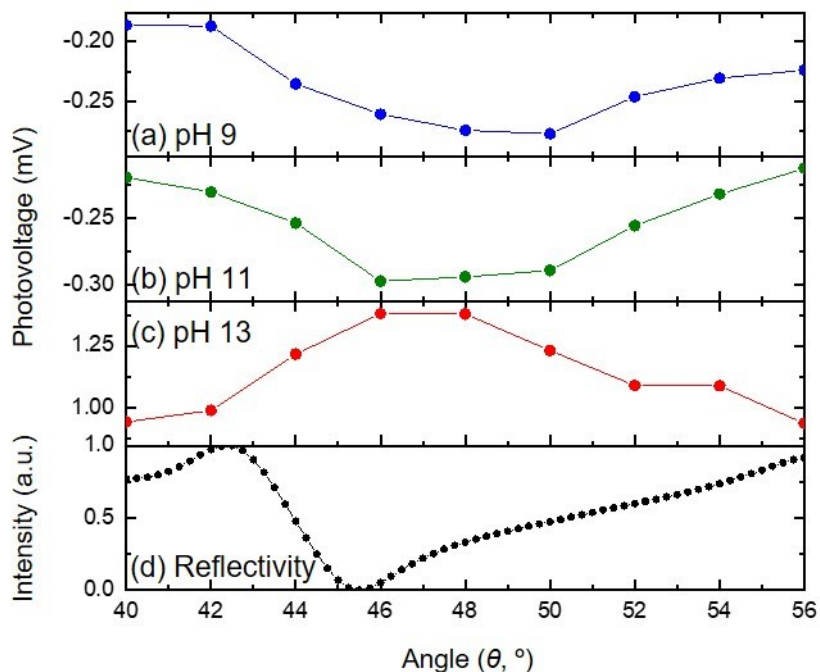


Figure S3. Solution pH-dependent photovoltage in a bare Au film. Photovoltages were measured while the incident angle of the 785 nm laser was tuned from 40 to 56° in solutions with pHs varied from (a) 9, (b) 11, and (c) 13 (three upper panels). Also shown is an angle-dependent reflectivity spectrum of a 40 nm-thick Au film measured at 785 nm (bottom panel). A less sensitive angle dependence in the photovoltage can be attributed to the increased illumination aperture size in order to obtain quantifiable photoelectrochemical signals in an oxide-free bare Au film.

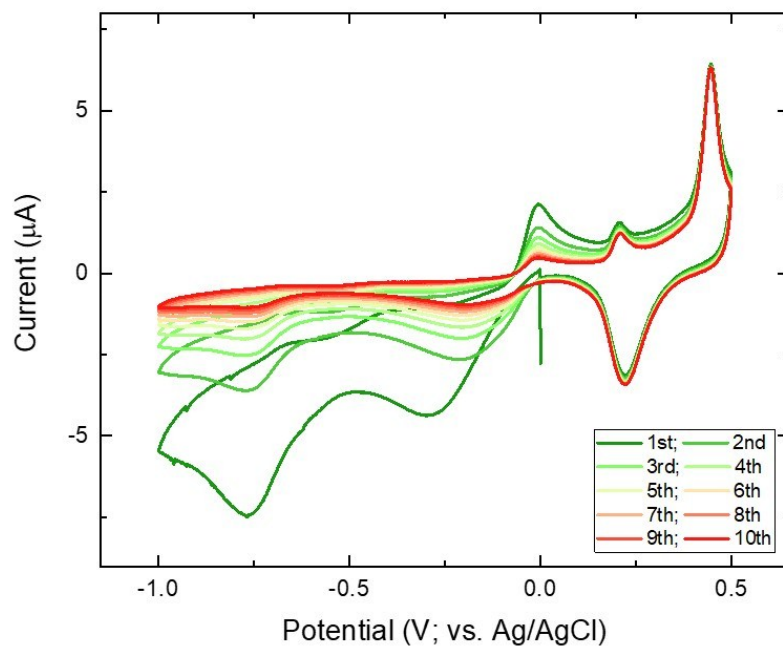


Figure S4. Cyclic voltammetry curves of a bare Au film. The Au film was interfaced with a de-aerated NaOH solution (0.1 M; pH 13). Cyclic voltammetry curves were measured in the dark, cycled 10 times at a scan speed of 50 mV/sec.

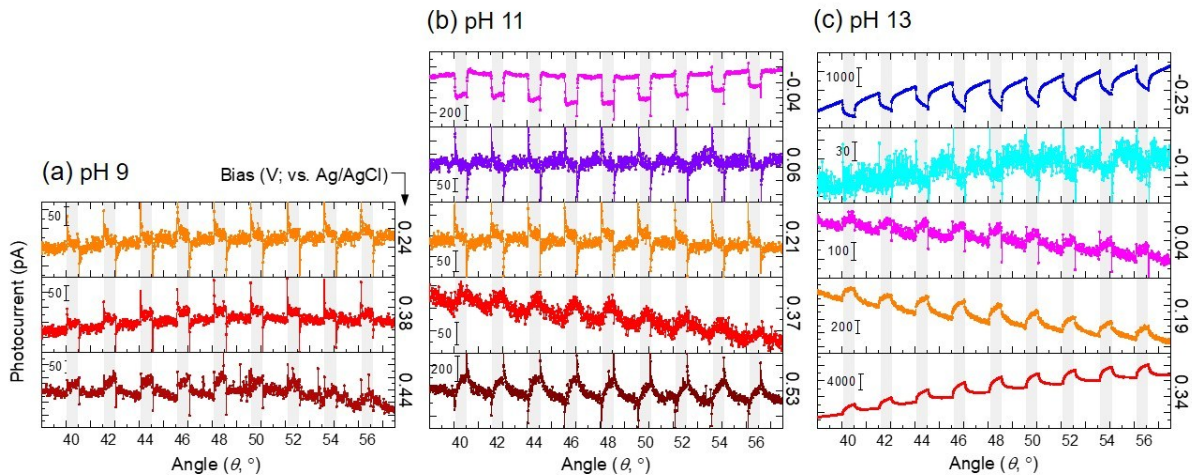


Figure S5. Dependence of photocurrents on solution pH and electrode potential in a bare Au film. Electrode potentials were varied for each measurement (labeled on right) with varied solution pH of (a) 9, (b) 11, and (c) 13, while the incident angle of light was continuously tuned from 40 to 56°.

References

- (1) T. P. White and K. R. Catchpole, *Appl. Phys. Lett.* 2012, **101**, 073905.
- (2) D. C. Ratchford, A. D. Dunkelberger, I. Vurgaftman, J. C. Owrutsky and P. E. Pehrsson, *Nano Lett.* 2017, **17**, 6047 – 6055.
- (3) I. Goykhman, B. Desiatov, J. Shappir, J. B. Khurgin and U. Levy, arXiv:1401.2624 2014.
- (4) A. M. Brown, R. Sundararaman, P. Narang, W. A. Goddard III and H. A. Atwater, *ACS Nano* 2015, **10**, 957 – 966.